

## FePt Thin Films Electrodeposited from Non-Aqueous Liquids

Zhou Hong-ru, Yu Yun-dan, Wei Guo-ying\*, Ge Hong-liang

College of Materials Science & Engineering, China Jiliang University, HangZhou 310018, China

\*E-mail: [guoyingwei@sina.com.cn](mailto:guoyingwei@sina.com.cn)

Received: 25 April 2012 / Accepted: 22 May 2012 / Published: 1 June 2012

---

FePt thin films have been electrodeposited from the mixture of ammonium hexachloroplatinate and iron dichloride in ionic liquids based on glycol and 1-Ethyl-3-methylimidazolium chloride. Electrochemical behaviour of iron dichloride in the liquids has been studied by cyclic voltammetry. The results show that the reduction of Fe (II) to Fe is irreversible diffused controlled and the diffusion coefficient is  $1.58 \times 10^{-7} \text{ cm}^2/\text{s}$ . The iron atomic content in the FePt films is ranging from 46.0 at % to 62.6 at % when deposition potentials have been changed from -1.4 V to -1.8 V vs Ag/AgCl in electrodeposition system with the ammonium hexachloroplatinate(50 mM/L), iron dichloride(550 mM/L), glycol and 1-Ethyl-3-methylimidazolium chloride at 373 K. The surface morphology of the deposited films was changed as the increase of deposition potential. A net-like structure appeared in FePt thin films with 52.5 at % iron. From the X-ray diffraction (XRD) pattern, it seems that the fct structural FePt has been obtained when the iron content is about 52.5 at %. Magnetic hysteresis loops show that the films exhibit ferromagnetic behaviors when the iron content in FePt films is 52.5 at % with the maximum coercivity 546 Oe.

---

**Keywords:** ionic liquids; cyclic voltammetry; electrodeposition; FePt; ferromagnetic

### 1. INTRODUCTION

FePt thin films have a universal use in national defense, medical treatment [1-6] due to their high coercivity and excellent chemical stability. As a perfect material in ultra-high density magnetic recording media, FePt in a bulk state has a large uniaxial magnetocrystalline anisotropy ( $K_u=6.6 \times 10^7 \text{ erg/cm}^3$ ) [7]. Chemical reduction, RF magnetron sputtering and thermal decomposition methods have been adopted generally to prepare FePt. The atom ratio of iron in FePt alloy is controlled about 50 at %

in the former researches to obtain good magnetic properties [8-16]. In the year of 2000, Sun et al used chemical reduction and thermal decomposition methods to synthesize FePt nano-particles. They found that there was a transformation of crystal structure in FePt from a face-centered cubic(fcc)phase(superparamagnetism) to a face-center tetragonal(fct)one(ferromagnetism)[8]. S.H. Sun group synthesized monodispersed 4 nm FePt magnetic nanoparticles by chemical method [17]. T .Shima et al succeeded in coeposition of Fe and Pt directly onto single crystalline MgO(001)in a high vacuum through multiple DC-sputtering. They investigated the magnetic domains of FePt[001]/MgO[001] films with 40 kOe when thickness is 10 nm [18]. Y.C. Wang et al. reported that ultrahigh coercivity of FePt films can restrict its application. They introduced a bilayered magnetic structure with an easy cost-effective micro/nanopattering of recording bits [19].

As mentioned above, FePt has been prepared by chemical reduction, magnetron sputtering, high temperature alloying or other methods. Electrodeposition is also used to prepare FePt films in aqueous solution because coatings can be obtained on the substrate with any shape. However, hydrogen evolution is the main hurdles to be overcome in industrialized production [20-21]. Hydrogen evolution during the electrodeposition in the aqueous electroplating solutions can influence the structure and properties of FePt thin films. Ionic liquid, as a perfect reagent with wide potential window, has a good high solubility of metal salts and high conductivity compared to non-aqueous solvents.

The use of ionic liquids heralds not only the ability to electrodeposit metals that have hitherto been impossible to reduce in aqueous solutions but also the capability to engineer the redox chemistry and control metal nucleation characteristics [22]. Recently, Hsin-Yi Huang et al studied the voltammetric behavior of Pt(II), Fe(II), and mixtures of Pt(II) and Fe(II) in ionic liquids [20]. They found that ionic liquids could have a good complexing effect on iron and platinum species, which suggested that codeposition of iron and platinum can be realized in ionic liquid systems without hydrogen evolution. We introduce an ionic liquid system with glycol(EG)and 1-Ethyl-3-methylimidazolium chloride(EMIC)dissolved ammonium hexachloroplatinate(Pt(IV))and iron dichloride(Fe(II))at 373 K. The electrochemical behavior of Fe(II)and Pt(IV)during deposition has been studied. Microstructure, surface morphology and magnetic properties of FePt thin films also have been discussed.

## 2. EXPERIMENTAL PART

### 2.1 Chemical Reagents

Composition and operating condition of FePt films were shown in Table 1, 1-Ethyl-3-methylimidazolium chloride(EMIC)was obtained from Alfa Aesar (Shanghai, China). glycol , ammonium hexachloroplatinate (Pt(IV)) and iron dichloride (Fe(II)) were bought from Shanghai July Chemical Co(Shanghai, China).

ITO conductive glass was utilized as the working electrode and platinum plate (99.95 %) was served as the counter electrode. Ag/AgCl(0.5 mm diameter) was chosen as the pseudo-reference electrode.

**Table 1.** Composition and operating condition of FePt films.

Component	Function	Content
1-Ethyl-3-methylimidazolium chloride (EMIC)	Complexing agents	50 mM/L
Glycol (EG)	Solvent	25 mL
Ammonium hexachloroplatinate (Pt(IV))	Source for Pt	50 mM/L
Iron dichloride (Fe(II))	Source for Fe	50 mM/L, 250 mM/L to 550 mM/L (100 mM/L apart)
Temperature	373 K	/

## 2.2 Electrochemical measurements

Electrochemical experiments were carried out in a nitrogen atmosphere glove box system filled with dry nitrogen. Voltammetric and electrodeposition were carried out in a three electrode system. ITO glasses were used as the working electrode (WE), one side of a glass plate was sealed, and the area of the other side exposed to solution was approximately 1 cm<sup>2</sup>. The counter electrode (CE) was a platinum plate (1 cm<sup>2</sup>) and the quasi-reference electrode was a Ag/AgCl wire (0.5 mm diameter). Electrolyte temperature was kept constant at 373 K by the oil bath during the electrochemical experiment process. Before every electrochemical experiment, the platinum working electrode was immersed in hydrochloric acid (1:1) for a few minutes, polished successively with increasingly finer grades of emery paper followed by silicon carbide grit, and finally to a mirror finish with aqueous slurry of 0.15 μm alumina, rinsed with distilled water, and dried under vacuum, the conductive glass plate was rinsed by the water and then cleared by the ethanol, reference electrode was calibrated before every experiment.

Cyclic voltammograms curve was recorded at the rate of 35 mV/s when the Pt(IV) /Fe(II) bath composition was 1(50 mM/L):1 with EG(25 mL) and EMIC(50 mM/L) at 373K. Different range of potentials from -1.4 V to -1.8 V vs Ag/AgCl were applied to make the FePt deposition with various bath composition(13:1(50 mM/L), 11:1, 9:1, 7:1 and 5:1) of Fe(II)/Pt(IV). After the electrodeposition , the films were immersed in oleic acid and protected in the nitrogen atmosphere glove box.

## 2.3 Apparatus details

All electrochemical measurements were conducted under nitrogen condition. Cyclic voltammetry (CV) and electrodeposition experiments were performed using a electrochemical system(PARSTAT 2273). The Fe and Pt elemental content and the thickness analysis of films were performed by EDX using Skyray (EDX-1800B). The magnetic properties of the films were measured

with vibrating sample magnetometer (VSM) (XPert Philips PW1830) at room temperature and their maximum applied fields were 10 kOe . The surface morphology of the sample was observed by a Hitachi (S-4700) scanning electron microscope (SEM). To determine the structure of films, x-ray diffraction (XRD) of Philips PW1830 with Cu-K $\alpha$  radiation was used.

### 3. RESULTS AND DISCUSSION

#### 3.1 Cyclic voltammetry in ionic liquids

##### 3.1.1 Electrochemical window

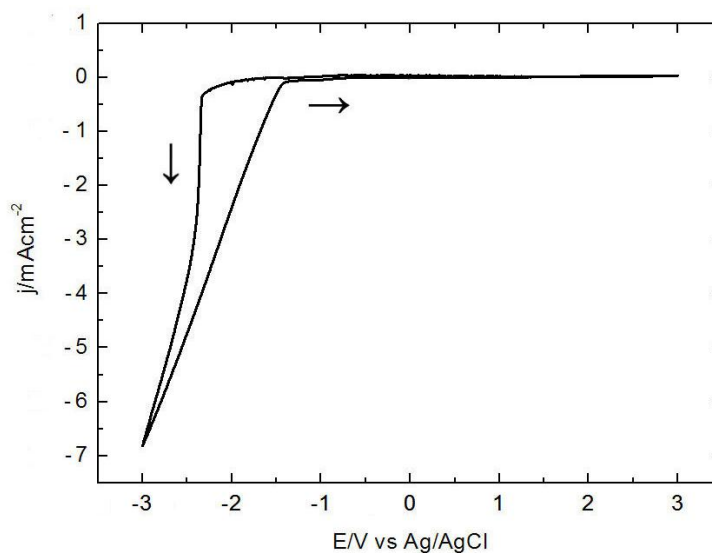


**Figure 1.** Cyclic voltammogram recorded at ITO glass electrode in 25 mL EG, 50 mM/L EMIC mixed ionic liquids. Temperature: 373 K. Scan rate: 35 mV/s.

The cyclic voltammogram of EG and EMIC mixed ionic liquids under the condition of 373 K and a linear scan rate of 35 mV/s were shown in Fig.1. No apparent oxidation peak and reduction peak were observed in the CV of the ionic liquids. The electrochemical window of the mixed liquids is about 4.5 V vs Ag/AgCl. The wide electrochemical window is not only conducive to later cyclic voltammogram but also helpful to the following electrodeposition.

##### 3.1.2 Cyclic voltammogram of Fe(II) (50 mM/L) and Pt(IV) (50 mM/L) in ionic liquids

The cyclic voltammetry behavior of the mixture of 50 mM/L Fe(II) and 50 mM/L Pt(IV) in ionic liquids (25 mL EG and 50 mM/L EMIC) is displayed in Fig 2. It is clear that the cyclic voltammogram exhibits two redox couples. The first couple in the center has two peaks. The reduction peak was due

to the bulk deposition of Pt and the anodic peak was due to stripping of the deposited Pt. The two peaks had good symmetry and the peak areas almost just the same. So few Pt remained on the ITO glass films ( $1\text{cm}^2$ ) after cyclic voltammetry experiment. The other couple also has two peaks, the reduction peak was due to the deposition of Fe and the anodic peak was due to stripping of the Fe. These two peaks have poor symmetry and reversibility. There was some iron remained on the ITO glass after cyclic voltammetry.

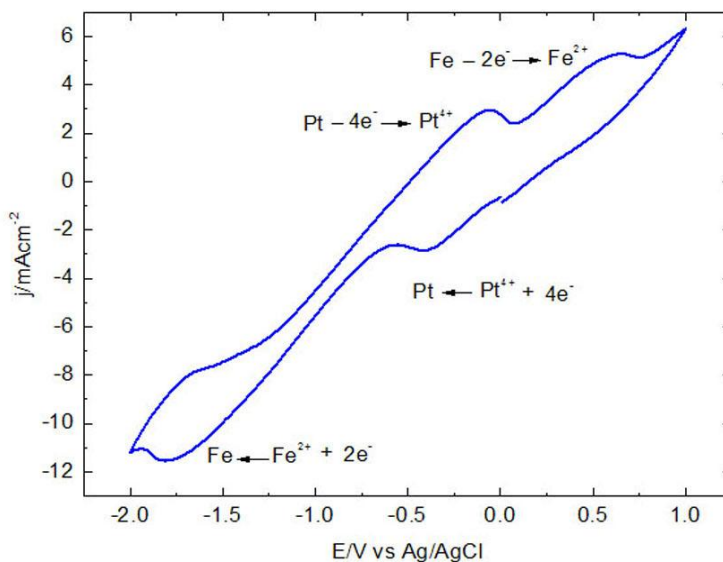
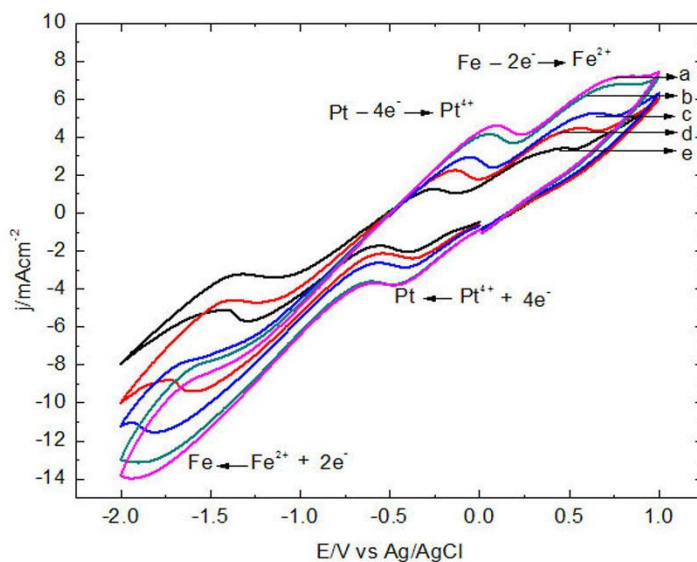


**Figure 2.** Cyclic voltammograms recorded at ITO glass electrode in ionic liquids (25 mL EG, 50 mM/L EMIC) containing 50 mM/L Pt(IV) and 50 mM/L Fe(II). Temperature: 373 K. Scan rate: 35 mV/s.

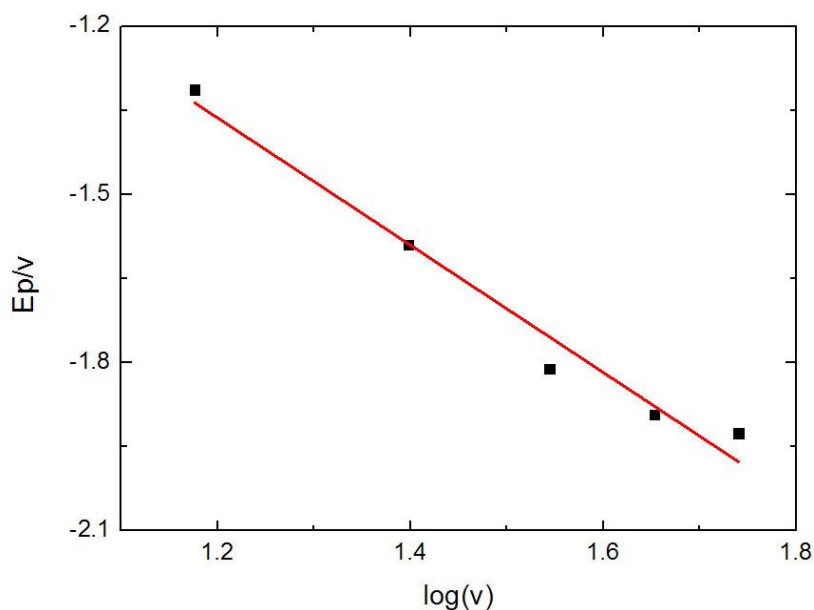
The reduction potential of Pt(IV) and Fe(II) are 0.71 V and -0.44 V vs NHE (normal hydrogen electrode) in the ionic liquids, respectively. The deposition potential difference between oxidation and reduction peaks is about 1.15 V vs NHE [23]. In Fig 2, Fe(II) and Pt(IV) deposition potentials were changed in ionic liquids. When the Fe (II) near the cathode was reduced that cathode needed quite a higher potential to further obtain Fe. In order to reduce the large difference of deposition potential for Fe(II) and Pt(IV) and realize the codeposition of Fe and Pt. The reversibility and diffusibility of iron ions in ionic liquids were studied.

Fig 3 shows the cyclic voltammograms when 50 mM/L Pt (IV) and 50 mM/L Fe(II) were added to ionic liquids (25 mL EG and 50 mM/L EMIC). The reduction peak of the Pt(IV) and Fe(II) was about  $-0.6\text{ V}$  and  $-1.8\text{ V}$  vs Ag/AgCl, respectively. The maximum of peak current density was decreased when the scan rates ( $\nu$ ) increased. The result indicates that the ionic liquids (EMIC) and metal cations (Fe(II)) formed a complex compound ( $\text{EMIFeCl}_3$ ), and provided evidence for the reduced metal cations activity in the electroplating solution [22,24]. With the increase of scan rate ( $\nu$ ), the

Fe(II)reduction peaks were more invisible and shifted negatively. This was due to the width of the electrochemical window's effect. At the slow scan rate ( $v$ ) the cyclic voltammograms shows more unsymmetrical peaks in Fig 3, suggesting that there was a self-inhibited process coincided at the initial growing region. With the scanning rate Fe(II)reduction peak became more negative, so the deposition progress of Fe(II)was irreversible [25].



**Figure 3.** Cyclic voltammograms of 50 mM/L Fe (II) and 50 mM/L Pt (IV) in ionic liquids (25 mL EG, 50 mM/L EMIC) with different scanning rates on a platinum electrode at 373 K: (a) 15 mV/s; (b)25mV/s; (c) 35 mV/s; (d) 45 mV/s and (e) 55 mV/s.



**Figure 4.** Peak potentials  $E_p$  vs  $\log v$  for the reduction of Fe (II) in ionic liquids (25 mL EG, 50 mM/L EMIC) at 373 K.

Cathodic peak potentials( $E_p$ )were obtained in the cyclic voltammograms in Fig 3. The cathodic peaks were widely separated as the result of the scan rates ( $\nu$ ) were changed. The cathodic peak potentials( $E_p$ )had a linear relationship with  $\log \nu$  in Fig 4, indicating that reduction of Fe (II) to Fe on a ITO glass electrode was an irreversible process.

The value of  $n_\alpha$  and  $|E_p - E_p/2|$  are according to the following Eq (1).

$$|E_p - E_p/2| = \frac{1.857RT}{\alpha n_\alpha F} \quad (1)$$

Where  $n_\alpha$  the number of electrons transferred,  $R$  the charge gas constant,  $F$  the Faraday constant and  $T$  the absolute temperature,  $\alpha$  the charge transfer coefficient. So the value of  $\alpha n_\alpha$  was found to be 0.28 at 373 K from Eq (1).

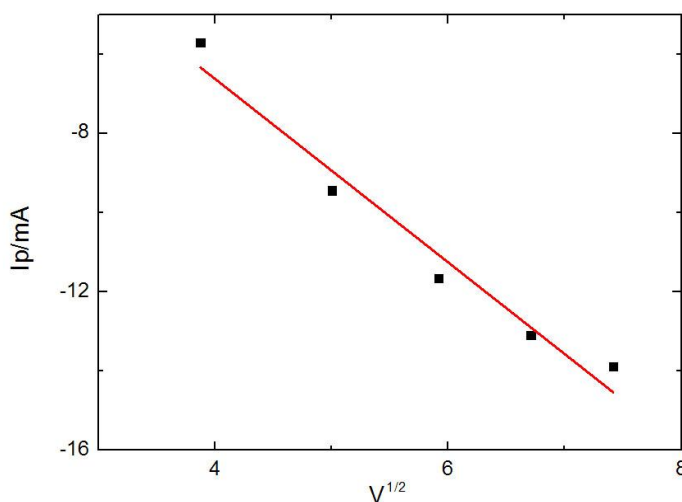


**Figure 5.** Peak currents  $I_p$  vs  $\nu^{1/2}$  for the reduction of Fe (II) in ionic liquids (25 mL EG, 50 mM/L EMIC) at 373 K.

In Fig 5, the  $I_p$  have a linear relationship with  $V^{1/2}$ . It can be indicated that the electrodeposition is determined by the diffusion process. The value of  $I_p$  and  $V^{1/2}$  are according to the following Eq (2).

$$I_p = 0.4958nF^{3/2}CAD_0^{1/2}\nu^{1/2}\left(\frac{\alpha n_\alpha}{R}\right)^{1/2} \quad (2)$$

where  $D_0$  the diffusion coefficient,  $\alpha$  the charge transfer coefficient,  $n_\alpha$  the number of electrons in the rate determining step,  $A$  the electrode area,  $C$  the ferrous ion concentration,  $n$  the number of exchanged electrons involved in the electrode process and  $\nu$  the potential scan rate.

The value of  $\alpha n_{\alpha} = 0.28$  can be obtained from Eq (1), using this value and the slope of the straight line obtained from the plot of  $I_p$  against  $v^{1/2}$  according to Eq (2), the diffusion coefficient of Fe (II) in ionic liquids (25 mL EG and 50 mM/L EMIC) was calculated.  $D_0$  value of Fe (II) in ionic liquids (25 mL EG and 50 mM/L EMIC) was  $1.58 \times 10^{-7} \text{ cm}^2/\text{s}$  at 373 K. Thus, it can be concluded from the above discussions that the reduction of Fe (II) to Fe was irreversible diffused controlled. In order to make the Fe(II)/Pt(IV) ions deposited at the same time and get the FePt alloy that iron atomic ratio next to 50 at%. In the following experiments, the bath composition of Fe(II)/Pt(IV) were controlled from 5:1(50 mM/L) to 13:1 in the ionic liquids (25 mL EG and 50 mM/L EMIC). From the Nernst equation, the reduction potential of Fe(II) and the atom ratio of iron on the films will be increased when the increase of the iron ion in ionic liquids.

### 3.2 Film composition, microstructure and magnetic properties of FePt thin films

#### 3.2.1 Film composition

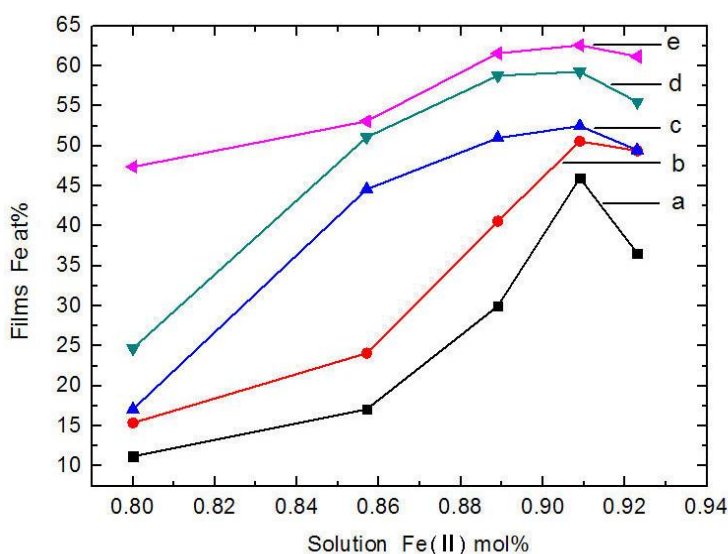


**Figure 6.** Effect of bath composition on the film composition: (a)  $E = -1.4 \text{ V}$ ; (b)  $E = -1.5 \text{ V}$ ; (c)  $E = -1.6 \text{ V}$ ; (d)  $E = -1.7 \text{ V}$  vs and (e)  $E = -1.8 \text{ V}$  vs Ag/AgCl with various bath composition (5:1(50 mM/L), 7:1, 9:1, 11:1 and 13:1) of Fe(II)/Pt(IV) in 25 mL EG and 50 mM/L EMIC.

The atom ratios of Fe and Pt in FePt thin films were detected by EDX. Fig 6 shows the variation of the atom ratios of Fe and Pt obtained from different composition of Fe (II) and Pt (IV) in the ionic liquids controlled by the deposition potential. It can be seen from Fig 6 that in the same bath composition of [Fe (II)/Pt (IV)] ionic liquids, the deposition potentials were controlled from -1.4 V to -1.8 V vs Ag/AgCl, the atom ratios of iron on the ITO glass electrode were tended to be increased. For the same deposition potential, when the [Fe (II)/Pt (IV)] bath composition were controlled from



5:1(50 mM/L) to 13:1, the atom ratios of Fe/Pt on the ITO glass electrode were increased and then reduced, there was a maximum atom ratio of Fe/Pt and the peak appeared when the bath composition of [Fe (II)/Pt (IV)] was 11:1(50mM/L).

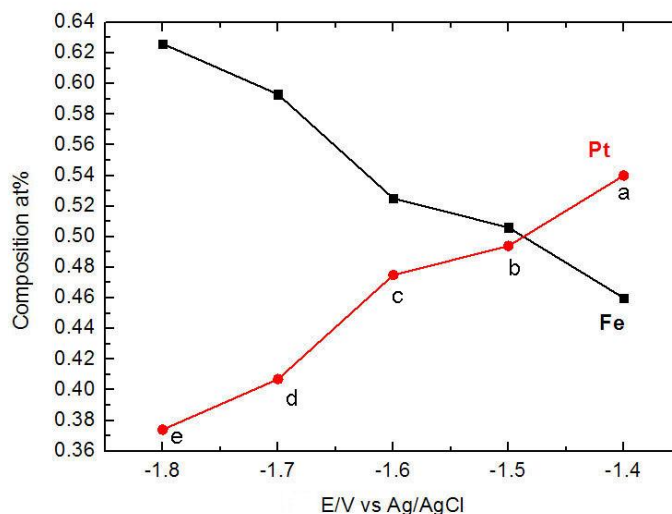


**Figure 7.** Effect of deposition potential on the film composition: (a) E=-1.4 V; (b) E=-1.5 V; (c) E=-1.6 V; (d) E=-1.7 V and (e) E=-1.8 V vs Ag/AgCl. Ionic liquids composition: 25 mL EG, 50 mM/L EMIC, and Fe (II)/Pt (IV) =11:1(50 mM/L).

It illustrated that, deposition potential was increased with Fe(II) concentration, and the Fe (II)/Pt (IV) ions were deposited at the same time when the deposition potential and concentration were suitable. Otherwise, when the Fe (II) concentration continued to be increased, the atom ratios of Fe/Pt on the films decreased. It illustrated that the electrostatic interaction of inter-ions increased when the iron ions increased. Fig 7 shows the atom ratios of iron on the ITO glass electrode from 46.0 at % to 62.6 at % when bath composition of Fe (II)/Pt (IV) was 11:1(50mM/L) in the ionic liquids. When deposition potential was -1.6 V vs Ag/AgCl, the atom ratio of iron was near to 50 at % on the ITO glass electrode. So the following experiments were focused on this section that the atom ratio of iron on the ITO glass electrode from 46.0 at % to 62.6 at % when bath composition of Fe (II)/Pt (IV) was 11:1(50mM/L) and the deposition potential were controlled from -1.4 V to -1.8 V vs Ag/AgCl in the ionic liquids (25 mL EG, 50 mM/L EMIC).

### 3.2.2 Morphology, microstructure and magnetic characteristics of FePt films

Fig.8 shows surface morphology of the FePt films deposited under different potentials on the glass substrate. As shown in Fig 8(a), the deposition films were covered by petal-like FePt crystals and

lots of needle-like different lengths FePt alloys structure also appeared. In Fig 8(b) to (e), due to the worse adhesion, more cracks appeared in FePt films. So with the continued increase of the deposition potential, the cracks were increased.

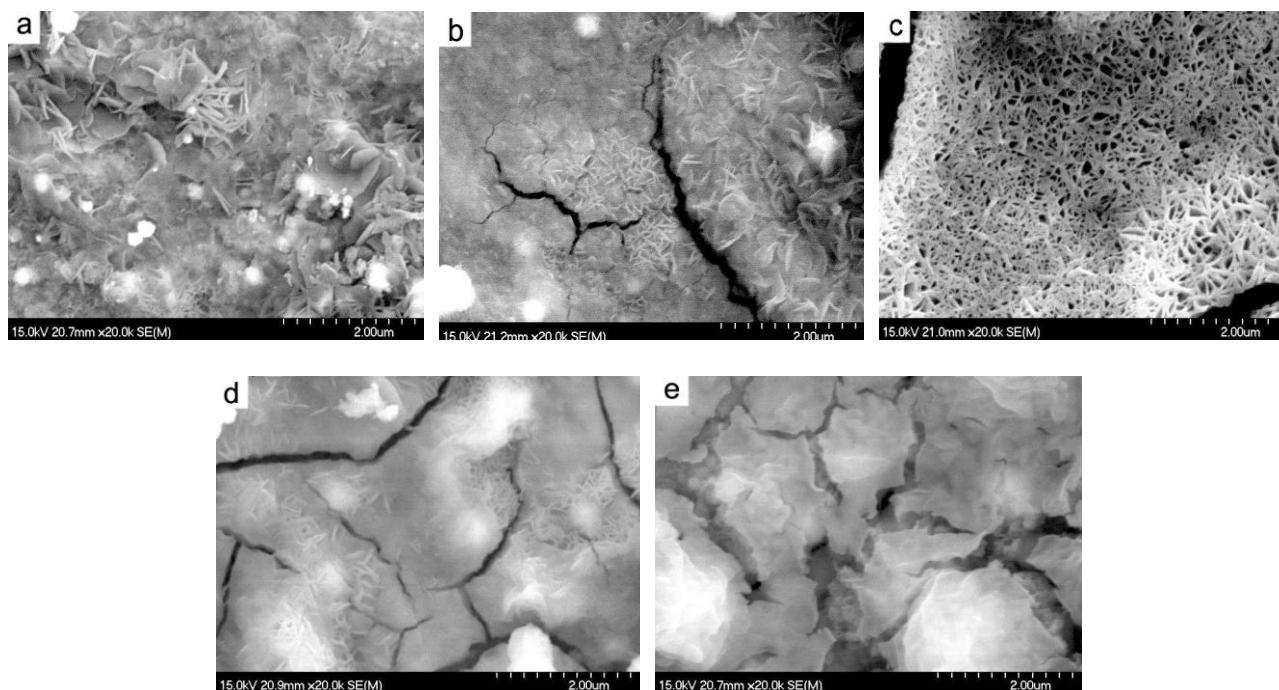
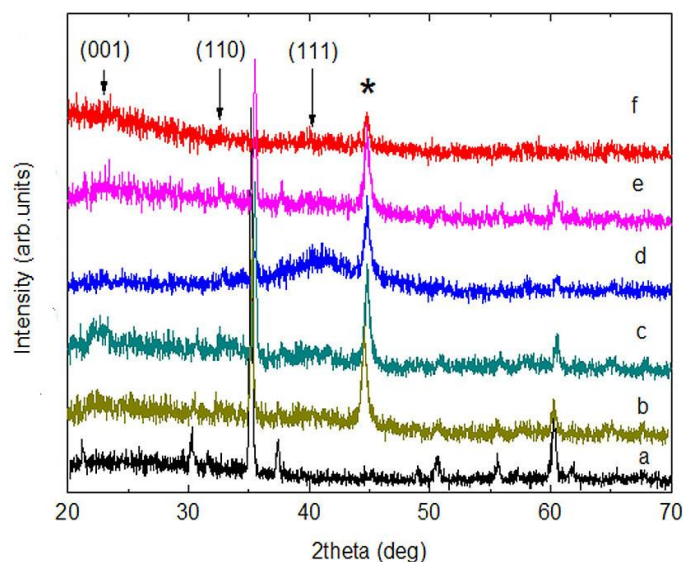


**Figure 8.** Surface morphologies of FePt thin films deposited under different potentials: (a)  $E = -1.4$  V vs Ag/AgCl, iron atomic percentage: 46.0 %; (b)  $E = -1.5$  V vs Ag/AgCl, iron atomic percentage: 49.7 at %; (c)  $E = -1.6$  V vs Ag/AgCl, iron atomic percentage: 52.5 at %; (d)  $E = -1.7$  V vs Ag/AgCl, iron atomic percentage: 59.3 at %; (e)  $E = -1.8$  V vs Ag/AgCl, iron atomic percentage: 62.6 at %. Temperature: 300 K

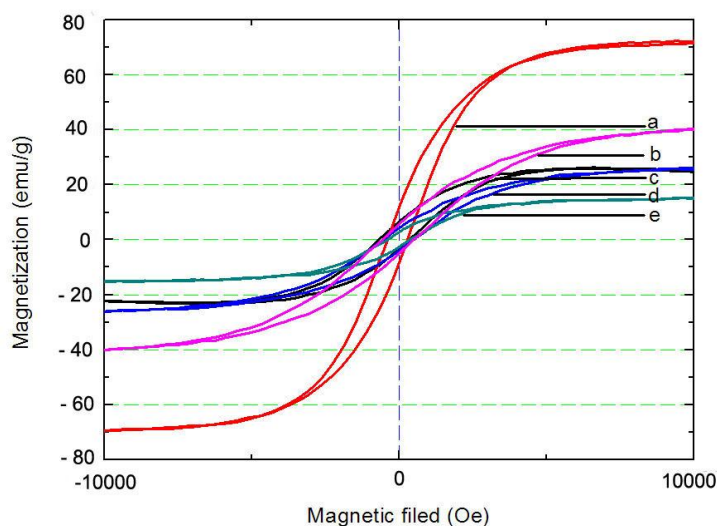
It revealed that the FePt thin films had poor adhesion with the increase of Fe(II) concentration in ionic liquids (25 mL EG, 50 mM/L EMIC). In Fig 8(b) to (c), needle-like FePt alloys structure were transformed into network structure when deposition potential was increased to  $-1.6$  V vs Ag/AgCl. In other words, a net-like structure appeared in FePt thin films with 52.5 at % iron.

Fig 9 shows the X-ray diffraction (XRD) pattern of the FePt films with different iron contents. The peaks noted “\*” represented the iron. In Fig 9(d), when the iron content was about 52.5 at %, there was a broad peak (111) at  $41^\circ$ . The weak FePt (001) at  $23^\circ$  and (110) at  $34^\circ$  peaks were hidden due to the broad (111) peak at  $41^\circ$ . In Fig 8(d), the intensities of superlattice peaks such as (001) and (110) were weak suggested that the electrodeposited FePt thin films had a partially ordered fct-structure [26, 27]. In Fig 9(b,c,e,f), no obvious fct characteristic peak appeared, the (111) peak was almost invisible. It seemed that the structural phase transformation from fcc to fct when the iron content was about 52.5 at % at 373 K in the ionic liquids. The X-ray diffraction pattern revealed that the fct phase FePt alloy

was hardly obtained when the iron content increased or decreased beyond 50 at % too much on the films.



**Figure 9.** X-ray diffraction patterns of FePt thin films with different iron contents: (a) the ITO glass substrate; (b)  $E=-1.4$  V vs Ag/AgCl, iron atomic percentage: 46.0 %; (c)  $E=-1.5$  V vs Ag/AgCl, iron atomic percentage: 49.7 at %; (d)  $E=-1.6$  V vs Ag/AgCl, iron atomic percentage: 52.5 at %; (e)  $E=-1.7$  V vs Ag/AgCl, iron atomic percentage: 59.3 at %; (f)  $E=-1.8$  V vs Ag/AgCl, iron atomic percentage: 62.6 at %. Temperature: 300 K.



**Figure 10.** Hysteresis loops of the different iron contents of the FePt films (a)  $E=-1.4$  V vs Ag/AgCl, iron atomic percentage: 46.0 at % (348 Oe); (b)  $E=-1.5$  V vs Ag/AgCl, iron atomic percentage: 49.7 at % (522 Oe); (c)  $E=-1.6$  V vs Ag/AgCl, iron atomic percentage: 52.5 at % (546 Oe); (d)  $E=-1.7$  V vs Ag/AgCl, iron atomic percentage: 59.3 at % (515 Oe); (e)  $E=-1.8$  V vs Ag/AgCl, iron atomic percentage: 62.6 at % (363 Oe). Temperature: 300 K.

Fig 10 shows magnetic hysteresis loops of FePt films with different iron contents at 300 K. As the iron contents of FePt films were increased from 46.0 at % to 62.6 at % as the coercivity was increased firstly and reduced afterward. When the iron content of FePt films was near 52.5 at %, the maximum coercivity was about 546.94 Oe. The hysteresis loops illustrated that the FePt films had ferromagnetic behavior, but just some nanoparticles larger than the mean diameter exhibited the ferromagnetic behavior and the fct phase FePt nanoparticles reached about certain diameter had the ferromagnetic behavior [8, 26, 28].

#### 4. CONCLUSION

The present paper shows that the electrodeposition of FePt thin films can be obtained with certain ratio of Fe(II)/Pt(IV) in ionic liquids electroplating bath (25 mL EG, 50 mM/L EMIC) and suitable deposition potential. The reduction of Fe (II) to Fe in the ionic liquids was irreversible controlled by diffusion. With the bath composition of Fe(II)/Pt(IV) was about 1(50 Mm/L):11 and deposition potentials were controlled from -1.4 V to -1.8 V vs Ag/AgCl, the atoms ratios of Fe/Pt films were increased from 46.0 at % to 62.6 at %. SEM micrographs shows needle-like FePt alloys structure was transformed into network structure when deposition potentials increased. With the increase of the iron content, the chasms were increased. It indicated that the cohesion of FePt films was not very well. From the X-ray diffraction patterns, the ferromagnetic FePt films were obtained when the atom ratios of Fe and Pt near 52.5 at %. The magnetic properties of FePt films could be optimized with the maximum coercivity of 546 Oe when the deposition potential is -1.6 V vs Ag/AgCl. The fct FePt with ferromagnetic behavior could be obtained through electrodeposition with deposition potential -1.6 V vs Ag/AgCl and certain bath composition(25 mL EG, 50 mM/L EMIC and bath composition of Fe(II)/Pt(IV) was 1:11 ) at 373 K.

#### ACKNOWLEDGEMENT

This research was supported by the National Natural Science Foundation (No. 21171155), International Science and Technology cooperation Program of China (No. 2011DFA52400) and Important Science and Technology innovation team of Zhejiang China (No.2010R50016).

#### References

1. R. Bernd, S. Sonja, A. Mehmed, F. W. Eberhard, *J. Magn. Magn. Mater*, 266 (2003)142
2. D. L. Leslie-Pelecky, R. D. Rieke, *Chem Mater*, 8(1996)1770
3. Xin. Gao, Kin Tam Dr, Kai Man Kerry Yu, Shik Chi Tsang Prof, *Small*, 1 (2005)949
4. Hui Wang, Shan Ji, Wei Wang, Vladimir Linkov, Sivakumar Pasupathi, Rongfang Wang, *Int. J. Electrochem. Sci*, 7(2012)3390
5. Eric G. Hope, James Sherrington, Aliso M. Stuart, *Adv. Synth. Catal*, 348 (2006) 1635

6. M. Vismadeb, Dr. Miaofang Chi, Dr. Karren L. MORE, Prof. Shouheng Sun, *Angew. Chem. Int. Ed.* 49 (2010)9368
7. D.Weller,A.Moser,L.Folks,M.E.Best et al, *IEEE Trans.magn*, 36(2000)10
8. S. Sun, C.B.Murray, D.Weller, L.Folks,A.Moser, *Science*, 287(2000)1989
9. S. Sun, *Adv. Mater*, 18(2006)393
10. T. Iwamoto, K. Matsumoto, Y. Kitamoto, N. Toshima, *Colloid Interface Sci*, 308(2007)564
11. A. Mougin, J. Ferre, O. Plantevin, et al, *J. Phys. D: Appl. Phys*, 43(2010)365002
12. T. L. Cheng, Y. Y. Huang, C. M. Rogers, et al, *J. Appl. Phys*, 107(2010)113920
13. C. Feng, E. Zhang, M. Y. Yang, et al, *J. Appl. Phy*, 107(2010)123911
14. W. B. Cui, X. H. Liu, F. Yang, et al, *J. Magn. Magn. Mater*, 322(2010)2027
15. F. Casoli, F. Albertini, L. Nasi, et al, *Acta Mate*, 58(2010)3594
16. M. Armand, F. Endres, D. R. MarFarlane, et al, *Nat. Mate*, 8(2009)621
17. S.H. Sun, S. Anders, T. Thomson, J. Baglin, M.F. Toney et al, *J. Phys. Chem. B*, 107 (2003)5419
18. 18.T .Shima, K .Takanashi, Y.K. Takanashi et al, *J. Magn. Magn. Mater*, 266(2003)171
19. Y.C. Wang, P. Sharma, A. Makino, *J. Phys.: Condens. Matter*, 24(2012)076004
20. Hsin-Yi Huang, Chung-Jui Su, Chai-Lin Kao, Po-Yu Chen, *J. Electroanal. Chem*, 650 (2010)1
21. Wojciech Simka, Dagmara Puszczczyk, Ginter Nawrat, *Electrochim. Acta*, 54(2009)5307
22. Andrew P. Abbott, Katy J. Mckenzie, *Phys. Chem. Chem.Phys*, 8(2006)4265
23. Alan Townshend, Colin F. Poole, Paul J. Worsfold, *Encyclopedia of Analytical Science*, Academic Press, (2005)
24. Q.G Zhang, J.Z Yang, X.M Lu, J.S Gui, M Huang, *Fluid Phase Equilib*, 226(2004)207
25. Caina Su, Maozhong An, Peixia Yang, Hongwei Gu, Xinghua Guo, *Appl. Surf. Sci*, 256(2010)4888
26. T.Iwamoto, K.Matsumoto, T.Matsushita, M.Inokuchi, N.Toshima, *Colloid Interface Sci*, 336(2009)879
27. F. Azarkharman, E.Saievare Iranizad, S.A.Sebt, *Appl. Surf. Sci*, 258(2012)5765
28. K.E. Elkins, T.S. Vedantam, J.P. Liu et al, *Nano Lett*, 3(2003)1647